

## Photovoltaic effects in BiFeO<sub>3</sub>

S. Y. Yang,<sup>1</sup> L. W. Martin,<sup>2,a)</sup> S. J. Byrnes,<sup>2,3</sup> T. E. Conry,<sup>1,2</sup> S. R. Basu,<sup>1</sup> D. Paran,<sup>1</sup> L. Reichertz,<sup>2</sup> J. Ihlefeld,<sup>4</sup> C. Adamo,<sup>4</sup> A. Melville,<sup>4</sup> Y.-H. Chu,<sup>5</sup> C.-H. Yang,<sup>3</sup> J. L. Musfeldt,<sup>6</sup> D. G. Schlom,<sup>4</sup> J. W. Ager III,<sup>2</sup> and R. Ramesh<sup>1,2,3</sup>

<sup>1</sup>Department of Materials Science and Engineering, University of California-Berkeley, Berkeley, California 94720, USA

<sup>2</sup>Materials Science Division, Lawrence Berkeley National Laboratory, Berkeley, California 94720, USA

<sup>3</sup>Department of Physics, University of California-Berkeley, Berkeley, California 94720, USA

<sup>4</sup>Department of Materials Science and Engineering, Cornell University, Ithaca, New York 14853, USA

<sup>5</sup>Department of Materials Science and Engineering, National Chiao Tung University, HsinChu 30010, Taiwan

<sup>6</sup>Department of Chemistry, University of Tennessee, Knoxville, Tennessee 37996, USA

(Received 25 April 2009; accepted 14 July 2009; published online 14 August 2009)

We report a photovoltaic effect in ferroelectric BiFeO<sub>3</sub> thin films. The all-oxide heterostructures with SrRuO<sub>3</sub> bottom and tin doped indium oxide top electrodes are characterized by open-circuit voltages  $\sim 0.8$ – $0.9$  V and external quantum efficiencies up to  $\sim 10\%$  when illuminated with the appropriate light. Efficiencies are at least an order of magnitude larger than the maximum efficiency under sunlight (AM 1.5) thus far reported for ferroelectric-based devices. The dependence of the measured open-circuit voltage on film thickness suggests contributions to the large open-circuit voltage from both the ferroelectric polarization and band offsets at the BiFeO<sub>3</sub>/tin doped indium oxide interface. © 2009 American Institute of Physics. [DOI: 10.1063/1.3204695]

Driven by the worldwide energy crisis, researchers have begun to investigate a broad spectrum of candidate materials for thin-film photovoltaic cells as an important step toward renewable energy production.<sup>1–3</sup> Oxide materials can be cheap, abundant, stable, and their properties (i.e., band gap, conductivity, etc.) can be systematically tuned through chemical substitutions, making them promising candidates for thin-film photovoltaics. Additionally, ferroelectrics present an alternative pathway for charge separation of photoexcited carriers. The photovoltaic properties of ferroelectric oxide ceramics were originally investigated over 30 years ago in numerous materials including LiNbO<sub>3</sub>,<sup>4–6</sup> BaTiO<sub>3</sub> (BTO),<sup>4</sup> and Pb(Zr,Ti)O<sub>3</sub> (PZT).<sup>7</sup> Much excitement was generated due to the anomalously large open circuit photovoltages, in some cases  $>10^4$  V, that were produced when the crystals were subject to illumination. It was concluded that the photovoltaic effect was a consequence of the non-centrosymmetry of the unit cell, which gives rise to asymmetries in electron excitation, relaxation, and scattering processes.<sup>4–7</sup> The photovoltaic efficiencies, however, were limited by small current densities (on the order of  $10^{-9}$  A/cm<sup>2</sup>) and the large band gaps (typically  $\sim 3.5$  eV) of these materials.

The photovoltaic properties of thin films of prototypical ferroelectrics, such as BTO and PZT, have been explored.<sup>8–11</sup> Recently the highest power-conversion efficiencies (0.28% for narrow-band ultraviolet light, which corresponds to  $\sim 0.005\%$  efficiency under sunlight) for ferroelectric thin films were reported in a La-doped PZT-based device.<sup>11</sup> The efficiency of such systems, however, remains small as a direct consequence of the relatively large band gaps of these materials although there have been proposed structures to address such limitations.<sup>12</sup> The emergence of lower band gap ferroelectrics oxides such as BiFeO<sub>3</sub> (BFO), offers an excit-

ing opportunity to explore new materials. Indeed reports of possible photovoltaic effects in BFO are just emerging.<sup>13</sup> The large saturation polarization ( $\sim 90$   $\mu\text{C}/\text{cm}^2$ ) in BFO thin films is quite robust and the band gap of BFO ( $E_g \sim 2.67$  eV) is smaller than many other ferroelectric perovskites.<sup>14,15</sup> In this letter, we report on photovoltaic devices based on BFO thin films that demonstrate the highest efficiency for a ferroelectric-based photovoltaic and represent an interesting alternative material class for study in pursuit of energy-related applications.

Epitaxial ferroelectric BFO thin films were grown by metal-organic chemical vapor deposition on (001) SrTiO<sub>3</sub> (STO) substrates with 50 nm epitaxial SrRuO<sub>3</sub> (SRO) bottom electrodes previously deposited by pulsed laser deposition. Films ranging in thickness from 50–1000 nm were deposited using a liquid precursor delivery system at 650 °C in 2 Torr flowing oxygen using Ar as a carrier gas, and were subsequently cooled to room temperature at the same pressure. Test structures were fabricated by sputtering 130 nm of the transparent conducting oxide tin doped indium oxide (ITO) at room temperature to create top electrodes with 50–500  $\mu\text{m}$  diameters.

Ferroelectric properties were characterized using a RT6000 tester (Radiant Technologies). Polarization-electric ( $P$ - $E$ ) field hysteresis measurements were performed in the range of frequencies between 100 Hz and 20 kHz. The current-voltage ( $I$ - $V$ ) behavior of the films in the dark and under illumination was characterized using a Keithley 230 voltage source and Keithley 6485 picoammeter. Light was applied using a 150 W Xe bulb to approximate the solar spectrum (AM 1.5). External quantum efficiency (EQE) measurements utilized a monochromator in series with the same light source and a lock-in amplifier coupled to a light chopper to measure the short-circuit current generated as a function of wavelength at zero applied bias.

<sup>a)</sup>Electronic mail: lwmartin@lbl.gov.

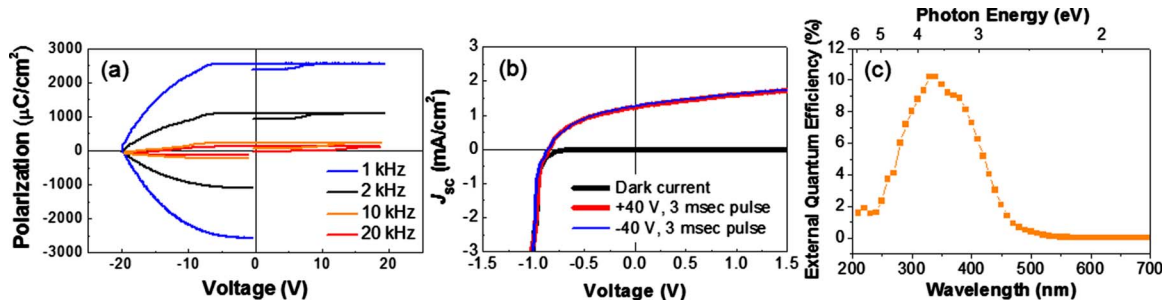


FIG. 1. (Color online) (a) Polarization-electric field hysteresis loops at various frequencies reveal diodelike behavior in one direction. (b) Light (red and blue) and dark (black curve, running through the origin)  $I$ - $V$  measurements completed at 2.85 suns intensity reveals photovoltaic effects in these device structures. There is no observed change in the light  $I$ - $V$  response upon application of an electric field. (c) Average EQE measurements for five different contacts on a single sample reveals efficiencies  $\sim 10\%$  under illumination with band gap light.

The high-quality epitaxial nature of the BFO thin films was confirmed by x-ray diffraction and only 00 $l$  diffraction peaks were observed indicating an epitaxial BFO thin film free of any secondary phases. Additionally, atomic force microscopy and PFM images reveal a smooth film surface with a homogeneous downward polarization and either a two or four-variant in-plane domain structure.<sup>16</sup> Optical absorption measurements reveal a direct band gap of  $\sim 2.67$  eV, in good agreement with previous results.<sup>12,13</sup>

Figure 1(a) shows a set of  $P$ - $E$  hysteresis loops as a function of test frequency. There are two noteworthy aspects of this data. First, the loops clearly show the existence of a ferroelectric hysteresis (that is further confirmed by pulsed polarization studies). Second, these measurements show the existence of a strong diodelike behavior, characterized by a large, directional leakage at negative voltages. that is strongly frequency dependent.  $I$ - $V$  curves taken in both the dark and under 285 mW/cm<sup>2</sup> white-light illumination reveal diodelike behavior and a photovoltaic effect [Fig. 1(b)]. The direction of short-circuit current flow was in all cases from the ITO, through the BFO, to the SRO. The thin-film BFO structures are distinguished by large open-circuit voltages ( $V_{OC}$ )  $\sim 0.8$ – $0.9$  V [ $\sim 16$ – $18$  kV/cm] for films thicker than 200 nm with short-circuit current densities ( $J_{SC}$ )  $\sim 1.5$  mA/cm<sup>2</sup>. It is noteworthy that this value of  $V_{OC}$  (and the corresponding electric field) is significantly higher than what has been previously reported for crystals [ $\sim 0.01$  kV/cm].<sup>12</sup>

EQE measurements, which quantify the  $J_{SC}$  as a function of the wavelength of incident light, give a better indication of the behavior of the devices when exposed to light adequate to promote charge excitation. Average EQE data for a set of five contacts on a wafer are shown in Fig. 1(c). A maximum conversion efficiency of  $\sim 10\%$  is observed when the light energy is larger than the band gap of BFO. The drop-off at the shortest wavelengths ( $< 325$  nm) is a result of light absorption in the ITO top contacts.

Armed with these observations of photovoltaic activity, we move to probe the origin of this photovoltaic effect. There are two likely scenarios that can explain the origin of the experimentally observed photovoltaic effect. The first involves the formation of a Schottky barrier at the BFO-electrode interface, a phenomenon that would depend on the nature of doping in BFO (i.e., the sign of the charge carrier). The second involves the role of the ferroelectric polarization as a driving force for charge separation within the device. In order to explore both possibilities, we first carried out careful, temperature-dependent (25–300 °C)  $I$ - $V$  measurements

of the same test structures (Fig. 2). For the entire temperature range, we were able to fit the  $I$ - $V$  data to a standard Schottky-diode model<sup>17</sup> (including a series resistance and a diode ideality factor of 2) and the results of these fits are shown for four illustrative  $I$ - $V$  curves (Fig. 2). The temperature dependence of the saturation current extracted from these Schottky fits is shown in a conventional Arrhenius-type plot (Fig. 2 inset). The fit of this data yields an interface offset potential  $\phi \sim 1.25$  eV. This interface potential at the electrode-ferroelectric interface (i.e., the ITO-BFO interface) causes band-bending at this interface, leading to the diodelike transport behavior that is captured in both the  $I$ - $V$  measurements as well as the ferroelectric hysteresis measurements (Fig. 1).

This potential at the ITO-BFO interface should lead to the formation of a depletion layer in the BFO. The width of this depletion layer in ferroelectric capacitor heterostructures has been predicted and measured to be of the order of several hundred nanometers for systems such as Pt-PZT and ITO-PZT.<sup>18,19</sup> Using the standard equation for the depletion layer width ( $W$ ) in ferroelectric semiconductors,

$$W = \sqrt{\frac{2\epsilon_0\epsilon\phi}{eN_D}}, \quad (1)$$

where  $\epsilon_0$  is the permittivity of free space,  $\epsilon$  is the dielectric constant of the semiconductor material,  $\phi$  is the Schottky barrier height, and  $N_D$  is the carrier density, we can calculate the depletion layer width at the interface, provided this parameters are known.<sup>20</sup> To estimate the carrier density in BFO ( $N_D$ ) frequency-dependent capacitance-voltage ( $C$ - $V$ ) measurements were carried out and Mott-Schottky plots were created by applying a 10 mV (rms) ac voltage superimposed on a dc voltage. By fitting the Mott-Schottky plots at 100 Hz, an ionizable impurity density of  $\sim 10^{17}$  cm<sup>-3</sup> ( $p$ -type in

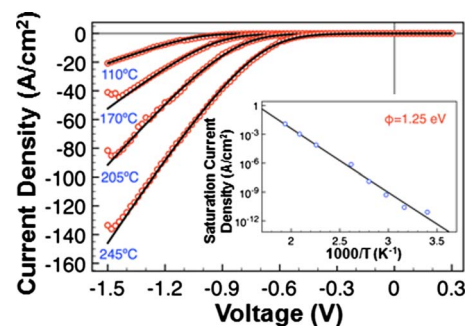


FIG. 2. (Color online) Temperature dependent  $I$ - $V$  measurements on ITO/BFO/SRO heterostructures. Inset, the Schottky modeling fitting of temperature dependent data reveals a Schottky barrier height of  $\sim 1.25$  eV.

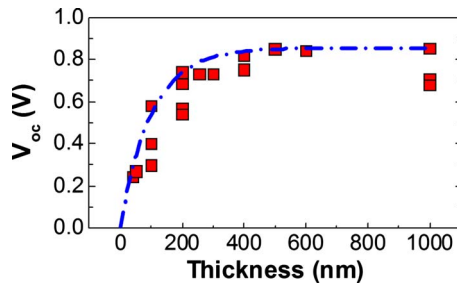


FIG. 3. (Color online)  $V_{OC}$  vs thickness for the ITO/BFO/SRO heterostructures reveals a decrease in  $V_{OC}$  in films less than  $\sim 300$  nm thick.

nature) and a Schottky barrier height of  $\sim 1.25$  eV was obtained. This suggests that Bi-vacancies are the likely source of extrinsic doping in this system. From this and assuming an experimentally measured dielectric constant of  $\sim 100$  (Ref. 21) we estimate the interface depletion layer width to be  $\sim 300$  nm, which is consistent with other estimates of depletion layers in ferroelectric capacitors.<sup>18</sup> These observations suggest that an interface depletion layer of the order of a few hundred nanometers could be the primary origin for the photovoltaic effect that is observed [Fig. 1(b)].<sup>22</sup> A corresponding thickness dependence of the  $V_{OC}$  is observed, with values reaching an apparent maximum of  $\sim 0.8$ – $0.9$  V for films of thicknesses greater than  $\sim 200$  nm (Fig 3). These observations would seem to suggest that the formation of a junction at the ITO-BFO interface is the primary mechanism responsible for the observed photovoltaic effect.

The question of whether the ferroelectricity has any role in determining the photovoltaic properties, however, remains unanswered. In an attempt to probe the role of ferroelectricity on this effect, we have completed photovoltaic measurements on 111-oriented BFO films. 111-oriented BFO films possess the strongest polarization along the direction of current flow (i.e., perpendicular to the film surface) and  $I$ - $V$  measurements show significantly different behavior (Fig. 4). First, the  $J_{SC} \sim 0.01$  mA/cm<sup>2</sup> which is approximately two orders of magnitude smaller than what is observed in the 001-oriented films. A potential origin for this difference is the intrinsic difference in domain structure between a 001- and 111-oriented BFO films. The 001-oriented films possess a network of  $71^\circ$  domain walls while the 111-oriented films are essentially single domain. Second, upon application of an electric field to switch the polarization state, we observed a corresponding reversible change in  $J_{SC}$  by approximately one order of magnitude. It has been reported that switching the polarization state in a metal-ferroelectric-metal capacitor

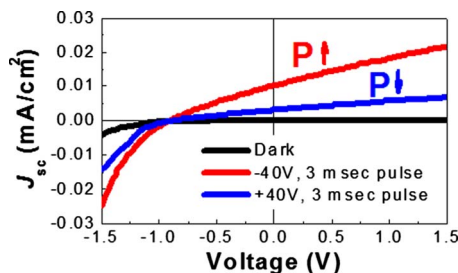


FIG. 4. (Color online) Light (red and blue) and dark (black)  $I$ - $V$  measurements for a ITO/BFO/SRO/STO(111) heterostructure reveals polarization dependent changes in the photovoltaic properties of the device.

structure with asymmetric contact potentials can lead to correspondingly asymmetric transport across the junction.<sup>23</sup> Finally, we observe little to no change in the magnitude of  $V_{OC}$  ( $\sim 1$  V) with polarization switching. Clearly more detailed studies are necessary to elaborate on the role of ferroelectricity in enabling this photovoltaic effect. In this regard, we note that switching the ferroelectric state of the BFO layer did not change the photovoltaic response or the nature of the diode ( $I$ - $V$  behavior).

In summary, photovoltaic behavior was demonstrated in all-oxide heterostructures of BFO with two conducting oxide electrodes. Devices are characterized by large  $V_{OC}$   $\sim 0.8$ – $0.9$  V and EQE  $\sim 10\%$ . The variation of  $V_{OC}$  with film thickness suggests a strong contribution from the interface depletion layer, but we cannot rule out an additional contribution from the ferroelectric polarization.

The work at Berkeley is supported by the Helios Solar Energy Research Center, which is supported by the Director, Office of Science, Office of Basic Energy Sciences of the U.S. Department of Energy under Contract No. DE-AC02-05CH11231. The work at Cornell is funded by the National Science Foundation through Grant No. DMR-0820404. The work at Tennessee is funded by the Materials Science Division, Office of Basic Energy Sciences, U.S. Department of Energy under Contract No. DE-FEG02-01ER45885. (S.Y.Y. and L.W.M. contributed equally to this work.)

<sup>1</sup>D. Ginley, M. A. Green, and R. Collins, *MRS Bull.* **33**, 355 (2008).

<sup>2</sup>I. Gur, N. A. Fromer, M. L. Geier, and A. P. Alivisatos, *Science* **310**, 462 (2005).

<sup>3</sup>B. O'Regan and M. Grätzel, *Nature (London)* **353**, 737 (1991).

<sup>4</sup>V. M. Fridkin and B. N. Popov, *Sov. Phys. Usp.* **21**, 981 (1978).

<sup>5</sup>A. M. Glass, D. von der Linde, and T. J. Negran, *Appl. Phys. Lett.* **25**, 233 (1974).

<sup>6</sup>A. M. Glass, D. von der Linde, D. H. Auston, and T. J. Negran, *J. Electron. Mater.* **4**, 915 (1975).

<sup>7</sup>P. S. Brody and F. Crowne, *J. Electron. Mater.* **4**, 955 (1975).

<sup>8</sup>V. S. Dharmadhikari and W. W. Grannemann, *J. Appl. Phys.* **53**, 8988 (1982).

<sup>9</sup>L. Pintilie, M. Alexe, A. Pignolet, and D. Hesse, *Appl. Phys. Lett.* **73**, 342 (1998).

<sup>10</sup>M. Ichiki, R. Maeda, Y. Morikawa, Y. Mabune, T. Nakada, and K. Nonaka, *Jpn. J. Appl. Phys., Part 1* **44**, 6927 (2005).

<sup>11</sup>M. Qin, K. Yao, and Y. C. Liang, *Appl. Phys. Lett.* **93**, 122904 (2008).

<sup>12</sup>P. S. Brody, U.S. Patent No. 4,326,938 (1980).

<sup>13</sup>T. Choi, S. Lee, Y. J. Choi, V. Kiryukhin, and S.-W. Cheong, *Science* **324**, 63 (2009).

<sup>14</sup>S. R. Basu, L. W. Martin, Y.-H. Chu, M. Gajek, R. Ramesh, R. C. Rai, X. Xu, and J. L. Musfeldt, *Appl. Phys. Lett.* **92**, 091905 (2008).

<sup>15</sup>A. J. Hauser, J. Zhang, L. Mier, R. A. Ricciardo, P. M. Woodward, T. L. Gustafson, L. J. Brillson, and F. Y. Yang, *Appl. Phys. Lett.* **92**, 222901 (2008).

<sup>16</sup>F. Zavaliche, S. Y. Yang, T. Zhao, Y.-H. Chu, M. P. Cruz, C. B. Eom, and R. Ramesh, *Phase Transitions* **79**, 991 (2006).

<sup>17</sup>S. M. Sze, *Physics of Semiconductor Devices: Physics and Technology*, 2nd ed. (Wiley, New York, 2001).

<sup>18</sup>C. J. Brennan, *Integr. Ferroelectr.* **2**, 73 (1992).

<sup>19</sup>C. J. Brennan, *Integr. Ferroelectr.* **9**, 335 (1995).

<sup>20</sup>H. Matsuura, *New J. Phys.* **2**, 8 (2000).

<sup>21</sup>J. Wang, Ph.D. thesis, University of Maryland, 2005.

<sup>22</sup>V. M. Fridkin, A. A. Grekov, E. A. Savchenko, and T. R. Volk, *Phys. Status Solidi A* **8**, K55 (1971).

<sup>23</sup>P. W. M. Blom, R. M. Wolf, J. F. M. Cillessen, and M. P. C. M. Krijn, *Phys. Rev. Lett.* **73**, 2107 (1994).